Physical, Mechanical, and Erosion Characterization of Palm Leaf Stalk Fiber Reinforced Epoxy Composites Filled with Palm Leaf Stem Stalk (PLSS) Powder

Jnanaranjan Kar,[a] Arun Kumar Rout,[b,*] and Alekha Kumar Sutar [a]

Palm-epoxy hybrid composites were fabricated by incorporating palm leaf stem stalk (PLSS) powder at levels of 0 wt%, 5 wt%, 10 wt%, and 15 wt%. Physical, mechanical, and erosion characteristics of these composites were investigated. Incorporation of filler powder had a positive effect on the hardness and impact strength and a negative effect on the tensile and flexural strength of the composites. The erosion test varied the impact angle (45° to 90°), impact velocity (40 m/s to 80 m/s), and erodent particle size (40 µm to 100 µm). The erosion experiments were statistically designed using Taguchi's orthogonal arrays. It was found that the erosion rate of palm-epoxy composites decreased with increasing filler powder content, and that the composite filled with 15 wt% PLSS had the highest erosion resistance. The surface morphology of the eroded samples were examined using scanning electron microscopy.

Keywords: Palm leaf stem stalk fiber; PLSS powder; Erosion wear; Mechanical properties

*Contact information: a: Department of Chemistry, Ravenshaw University, Cuttack, India, 753001; b: Department of Production Engineering, Veer Surendra Sai University of Technology, Burla, India, 768018; *Corresponding author: arun.rout.6314@gmail.com*

INTRODUCTION

Over recent decades, plant-based fibers are slowly replacing conventional synthetic fibers in polymer matrices due to their low cost, biodegradability, low density, and high aspect ratio for effective stress transfer (Fung *et al*. 2003; Paul *et al*. 2003; Ku *et al*. 2011). It has been proposed that composites made with reinforcing natural fibers can be modified to produce lightweight, low cost, and nonhazardous materials. Plant-based fibers such as jute, bamboo, sisal, oil palm, flax straw, and banana have been successfully implemented as reinforcing fibers in polymer composites. In spite of several advantages, natural fiber has some limitations, including high moisture absorption (hydrophilic), high resin consumption, and high shrinkage, which lead to surface cracking and de-bonding between the matrix and the reinforcing fibers (Dhakal *et al*. 2007; John *et al*. 2008). The above limitations may be reduced by utilizing various chemical pre-treatments of the natural fibers before use.

Many researchers have reported that chemically-treated fiber-reinforced composites have shown improved mechanical and thermal properties, in addition to lower moisture absorption, than the composites made with the untreated fibers. Alkali has been used as a pretreatment in many plant-based fibers used in composites (Balaji and Nagarajan 2017; Manimaran *et al*. 2018). A 5% alkali treatment of borassus fruit fibers resulted in higher tensile strength compared to the control without treatment (Boopathi *et al*. 2012). Alkali treatment removes the noncellulosic constituents from the natural fibers (Obi Reddy

et al. 2013; Rout *et al*. 2016). Similarly, a polyvinyl chloride (PVC) composite made with sorghum straw fiber as a reinforcing agent exhibits high tensile and erosion resistance behavior when the straw fibers are treated with 4.5% NaOH (Jiang *et al.* 2018).

Fiore *et al*. (2015) reported that alkali-treated kenaf fibers incorporated in an epoxy composite have a negative impact on the fibers' strength when they are treated with 6% NaOH for 48 h. Swain and Biswas (2017) compared the influence of NaOH and benzoyl chloride treatments on jute fibers used in epoxy composites. The authors confirm that chemically-treated fibers result in improved mechanical properties of the composites compared to untreated fibers. However, composites made with fibers treated by benzoyl chloride had higher resistance to water absorption.

Joseph *et al.* (1996) investigated the effects of different chemical pretreatments of short sisal fiber on the tensile properties of polyethylene composites made from these fibers. The investigators found that the composite's tensile strength was improved with the surface modifications of the fibers *via* chemical treatment. Sisal fibers treated with peroxide had better interfacial adhesion to the polyethylene matrix. Similarly, Liu *et al*. (2014) modified the surfaces of abaca fibers with alkali and silane. They reported that chemically treated abaca-epoxy composites had shown better tensile properties than the untreated ones.

Composites repetitively used in the hostile environment of a workplace or process as structural and engineering components undergo solid particle erosion wear. Solid particle erosion is the elimination of material from the upper surface that arises due to the frequent impact of small solid particulates and it causes surface degradation, surface roughening that reduces the functional life of the composite (Tewari *et al*. 2002). Examples of such erosion cases can be found with aircraft engine blades, pipelines carrying sand slurries, and helicopter rotor blades. Hence, it became an important issue to minimize the erosion rate of the composite material before it is used in any engineering application. Several investigations have studied the effect of different parameters on erosion resistance of composites filled with reinforcing fiber.

Rout and Satapathy (2012) examined the mechanical and erosion resistance of rice husk reinforced glass-epoxy composites. The authors employed an experimental approach using Taguchi orthogonal arrays. They concluded that the erosive resistance of glass-epoxy composites increased with the inclusion of rice husk filler particles and that composites containing 15 wt% rice husk exhibited maximum erosion resistance.

Zhang *et al*. (2016) investigated the tribological mechanisms of silica nanoparticle filled epoxy composites reinforced with carbon nanotubes (CNTs), short carbon fibers, and short glass fibers. The authors reported that silica addition reduced the wear rate of CNT-reinforced epoxy composites. Mohan *et al*. (2013) investigated the erosive wear of tungsten carbide (WC) filled glass-epoxy composites at impingement angles of 30° to 90° and impact velocities of 40 m/s to 80 m/s. The authors observed that composites filled with WC exhibited a lower erosion rate when compared to composites made without WC filler. In another study, Panda *et al*. (2014) investigated the erosion wear of a glass-epoxy-aluminum nitride (AIN) hybrid composite. The specific wear of the composite specimen was examined by varying different parameters. The authors observed that filler addition has a positive effect on the hardness and erosion resistance, and a negative impact on the tensile strength of the glass epoxy composite.

Moreover, many investigators have also reported the effect of natural fibers on the erosive characterization of various polymer composites. An erosive study of *Luffa cylindrica*-epoxy composite was conducted by Mohanta and Acharya (2015) in which the erosion rate was evaluated under various testing conditions. The authors observed that the erosion rate increased with increasing velocity of the impinging particles. Similarly, Biswas and Satapathy (2009) compared the erosion characteristics of bamboo-epoxy and glass-epoxy composites filled with red mud; the experimental design that examined different test conditions was based on Taguchi orthogonal arrays. The investigators found bamboo-epoxy composites filled with red mud exhibited better wear resistance than glass-epoxy composites under similar testing conditions.

Das and Biswas (2017) examined the erosive wear of coir-epoxy composites filled with alumina. The investigators reported that the composites filled with alumina particles had better erosion resistance behavior than the composites without filler. The erosion resistence of bamboo-epoxy composites filled with copper slag particles has been investigated (Biswas 2014). The significant factors that affected composite erosion efficiency were analyzed by an ANOVA. It was reported that the factors, such as impingement angle, impact velocity, and fiber loading percentage, had a greater influence on the erosion rate.

Similarly, Jena *et al.* (2016) studied the solid particle erosion behavior of bamboo-epoxy composites filled with cenosphere. The erosion experiments were conducted at different impact velocities and impingement angles. The authors reported that the composites filled with cenosphere had better erosion resistance than the composites without cenosphere filler. Sarkar *et al*. (2017) investigated the mechanical, thermal, and erosion properties of a polypropylene (PP) composite made with acrylic modified coconut fibers. The authors reported that chemically modified fibers improved the mechanical, thermal, and wear resistance properties of the polypropylene composites compared to the control composites made with unmodified fibers. Mohanty (2017) investigated the solid particle erosion performance of date palm leaf (DPL)-polyvinyl pyrrolidone (PVP) composites. The experiments were performed with various impingement angles (15° to 90°) and impact velocities (48 to 109 m/s). The author observed that polyvinyl pyrrolidone composites had a higher erosion rate at 30° impingement angles, whereas PVP/DPL composites exhibited a higher erosion rate at 45° impingement angles that were irrespective of fiber loading.

Although a good amount of research is available on erosion study of both synthetic and natural fiber reinforced composites, there is no information regarding the erosion wear performance of composites reinforced with palm tree leaf stalk fiber, and filler with palm leaf stem stalk (PLSS) powder. Such fiber is obtained from the leaf stalk of a palm tree. It consists of cellulose, hemicelluloses, lignin, and waxes. It was reported earlier that when these fiber are alkali treated, the fibers became rough due to the removal of hemicelluloses, lignin, and waxes, which was confirmed by scanning electron microscopy (SEM), X-ray diffraction (XRD), Fourier transform infrared (FTIR), and solid state nuclear magnetic radiation (NMR) analyses (Rout *et al*. 2016). The alkali treatment led to improved fiber-matrix adhesion, fiber wetting, and mechanical strength. Therefore, the purpose of this study is to create a low-cost hybrid palm-epoxy composite filled with PLSS powder, and to analyze the composite's physical, mechanical, and erosion behaviors for potential engineering applications

EXPERIMENTAL

Materials

In this study, palm leaf stalk was used as the reinforcement fibers, and epoxy (LY556) and hardener HY-951 were used as the composite matrix components. The matrix components were supplied by Hindustan Ciba-Geigy India Ltd. (Kolkota, India). The main features of the epoxy resin are its excellent thermal and corrosion resistance properties. The palm leaf stalks were collected from village Baramba, Cuttack, Odisha, India. First, the thorns on both sides of the leaf stalk were separated and then the fibers were separated from the stalk using a knife. The collected fibers were then air-dried in daylight for 4 to 5 days to reduce their moisture content.

Alkali treatment

Based on the authors' previous work (Rout *et al*. 2016), fiber pretreated with 5% alkali for 6 h exhibited better mechanical properties and had the highest cellulose content compared to the other treatment times (Rout *et al*. 2016). Hence, the fibers used in this study were treated with 5% NaOH for 6 h. The pretreated fibers were cut with scissors to form a fiber mat with the dimensions of 200 mm × 5 mm × 0.4 mm.

Composite fabrication

Bi-directional palm fiber mats were fabricated consisting of palm fibers, epoxy, and PLSS powder by varying the filler content (0 wt%, 5 wt%, 10 wt%, and 15 wt%) to formulate the composites C_1, C_2, C_3, and C_4, respectively (Table 1). All composites were prepared by using the simple hand-lay-up method. Initially, silicone gel was uniformly sprayed onto both sides of the mold (250 mm × 10 mm × 5 mm). Then, each palm fiber mat was pre-impregnated with the resin matrix. Each composite sample was pressed with 30 kg force for 12 h. Next, the sample was removed from the mold and post-cured at ambient conditions for another 12 h. Finally, the samples were cut into suitable dimensions for mechanical and wear tests.

Table 1. Designation and Composition of Composite Samples

Sample No	Composition	Designation
1	70 wt% Epoxy + 30 wt% palm fiber + 0 wt% PLSS powder	C_1
2	65 wt% Epoxy + 30 wt% palm fiber + 5 wt% PLSS powder	C_2
3	60wt% Epoxy + 30 wt% palm fiber + 10 wt% PLSS powder	C_3
4	55wt% Epoxy + 30 wt% palm fiber + 15 wt% PLSS powder	C_4

Methods

Test Apparatus- Density

The theoretical densities of the developed composites (C_1, C_2, C_3, and C_4) were calculated as per Eq. 1 (Agarwal and Broutman 1990),

$$\rho_{ct} = \frac{1}{\left(\frac{W_f}{\rho_f}\right)+\left(\frac{W_m}{\rho_m}\right)+\left(\frac{W_p}{\rho_p}\right)} \quad (1)$$

where W and ρ represent the weight fraction (gm/gm) and density (gm/cm^3), respectively. The subscripts f, m, p, and ct indicate the palm fiber, the epoxy matrix, filler powder, and the composite, respectively.

However, the actual density of the composite was calculated utilizing the Archimedes Principle. The dissimilarity between the actual density (ρ_{ce}) and the theoretical density (ρ_{ct}) represents the void content (V_v), which is calculated by Eq. 2:

$$V_v = \left(\frac{\rho_{ct} - \rho_{ce}}{\rho_{ct}} \right) \quad (2)$$

Microhardness test

The microhardness of the composites was measured using a Micro-Vickers hardness tester (LV700, LECO Co., Michigan, MI, USA) according to ASTM E384-11e1 (2011). A load of 24.54 N was applied to the sample for 20 s to determine its hardness.

Tensile test

The tensile strength of the composites was measured using a universal testing chine (Instron 3369; Instron India Pvt. Ltd., Chennai, India) with a gauge length of 50 mm and at a crosshead speed of 2 mm/min. The measurements were conducted in accordance to the ASTM D3039M-14 (2014) standard. Each sample (150 mm × 25 mm × 4 mm) was tested five times, and the average of the replicates was taken as the sample's tensile value.

Flexural test

The flexural strength of the composites was measured using the Instron 3369 universal testing machine. The test specimens were prepared in accordance to the ASTM D790-03 (2003) standard, with the dimensions of 100 mm × 15 mm × 4 mm. The flexural strength (FS) of the composite was computed as,

$$FS = \left(\frac{3PL}{2bt^2} \right) \quad (3)$$

where P, b, t, and L are the maximum load (N), the width (mm), the thickness (mm), and the span length (mm) of the test sample, respectively.

Impact energy absorption

The impact strength of the composite specimens with dimensions of 66 mm × 13 mm × 4 mm was measured using an IZOD impact tester (Veekay Test Lab, Mumbai, Maharashtra, India). Measurements were performed in accordance to the ASTM D256-10 (2010) standard. The testing samples were mounted into the impact testing machine and the energy absorbed during each test was calculated. Each specimen was tested five times, and the average of these values was taken as the impact strength value.

Solid particle erosion test

An erosion test apparatus (TR-470; Ducom Instruments Ltd., Bangalore, India) was used to measure the erosion of the composite specimens in accordance to the ASTM G76-13 (2013) standard. Dry alumina erodent was passed from the hopper by gravity through a conveyor belt system (3 mm/min) into an air erodent mixing chamber. Then, the mixture was accelerated by passing it through a convergence nozzle, where the stream strikes the

composite specimen. Dry alumina particles with sizes of 40 μm, 60 μm, 80 μm, and 100μm impinged the surface of the specimens (25 mm × 25 mm × 4 mm) at angles of 45°, 60°, 75°, and 90°.

Scanning electron microscopy

The surface morphology of the eroded specimens was observed using a scanning electron microscope (SEM) model JEOL JSM-6480 LV (JEOL Ltd., Tokyo Japan).

Statistical Experimental Design

A Taguchi experimental design is a systematic statistical approach used to optimize performance, quality, and cost. Prior to employing this approach, the number of parameters affecting the optimization needs to be narrowed to eliminate insignificant effects. The scientific literature indicates that the erosion behavior of composite samples principally depends upon erodent impact velocity, impingement angle, and particle size, in addition to composite filler content (Patnaik *et al*. 2010). The influences of these four parameters were examined in this study utilizing a L_{16} orthogonal array design. Details of the experimental design are given in Table 2.

In a conventional full-factorial statistical design, 256 runs (= 4^4) are required to examine the four parameters at four different levels. The number of runs can be reduced to 16 runs by utilizing a Taguchi experimental approach. The obtained experimental data are converted into signal-to-noise (*S/N*) ratios. However, the S/N ratios were different for different test runs. Therefore, 'smaller is better' characteristics were chosen for the minimum erosion rate as per Eq. 4,

$$SN = -10\log_{10}\left(\frac{1}{n}\sum_{i=1}^{n} y_i^2\right) \quad (4)$$

where *n* is the number of observations and *y* is the observed value.

The control factors, along with their corresponding levels, are shown in Table 3. The rows represent different test condition levels and the columns (second to fifth) represent the test parameters. The column is assigned to the filler content (A), the impact velocity (B), the impingement angle (C), and the erodent size (D). The statistical analysis of erosion wear has been conducted using MINITAB 16 software (Minitab Ltd., Brandon Court, UK).

Table 2. Setting of Parameter

Control Factors	Symbols	Fixed Parameters
PLSS content	A	Erodent feed rate (g/min), 10 ± 1.0
Impact velocity	B	Erodent, alumina
Impingement angle	C	Nozzle diameter (3 mm)
Erodent size	D	Length of the nozzle (80 mm), Standoff distance (100 mm)

Table 3. Control Factors and Their Selected Levels

Control Factors	I	II	III	IV	Units
Filler content	0	5	10	15	wt%
Impact velocity	40	50	60	80	m/s
Impingement angle	45	60	75	90	Degree (°)
Erodent size	40	60	80	100	mm

Table 4. Orthogonal Array for L_{16} Taguchi Design

Test Run	A: Filler Content (wt%)	B: Impact Velocity (m/s)	C: Impingement Angle (°)	D: Erodent Size (µm)	E_r: Erosion Wear Rate (mg/kg)	*S/N* Ratio (dB)
1	0	40	45	40	282.45	-49.0188
2	0	50	60	60	375.12	-51.4834
3	0	60	75	80	407.65	-52.2057
4	0	80	90	100	551.24	-54.8268
5	5	40	60	80	272.37	-48.7031
6	5	50	45	100	320.19	-50.1081
7	5	60	90	40	401.27	-52.0687
8	5	80	75	60	450.32	-53.0704
9	10	40	75	100	342.56	-50.6947
10	10	50	90	80	386.88	-51.7515
11	10	60	45	60	310.82	-49.8501
12	10	80	60	40	455.23	-53.1646
13	15	40	90	60	398.67	-52.0123
14	15	50	75	40	423.16	-52.5300
15	15	60	60	100	512.37	-54.1917
16	15	80	45	80	480.11	-53.6268

RESULTS AND DISCUSSION

Physical Properties

Density

Density is one of the key parameters generally used for judging the quality of a composite. The void content is the difference between the measured and the theoretical density of the composite. Higher void contents generally represent lower strength and higher water absorbtivity (Rout and Satapathy 2013). A good composite should have lower amounts of voids. However, some void content is unavoidable in composites developed by the hand-lay-up technique.

Table 5 shows the experimentally and theoretically measured densities of all tested composite samples along with the void content. It was noticed that both densities were different. The difference conveys the void content and pores in the composite. Composite C_1 had negligible void content due to the absence of PLSS powder in the composite (Table 5). With the addition of PLSS powder, the void content of specimens increased from 1.08 wt% to 4.54 wt%.

Table 5. Theoretical and Measured Densities of PLSS Filled Palm-epoxy Composites

Composite	Measured Density (gm/cc)	Theoretical Density (gm/cc)	Volume Fraction of Voids (%)
C_1	1.107	1.095	1.08
C_2	1.097	1.072	2.27
C_3	1.087	1.051	3.31
C_4	1.077	1.028	4.54

The composites with 15 wt% PLSS had a higher amount of voids. This may have been attributable to the entrapped air at the filler-matrix interfaces that occurred during mixing. Similar results have been reported earlier by Rout and Satapathy (2012) for glass-epoxy composites with rice husk filler, and Swain and Biswas (2017) for jute-epoxy composites with alumina as filler.

Microhardness

The hardness of palm-epoxy composites filled with PLSS is shown in Fig.1. The hardness increased from 36 Hv to 45 Hv with the increase in PLSS content from 0 wt% to 15 wt%. Similar observations have been reported in previous literature (Rout and Satapathy 2012; Prabhu *et al*. 2017; Swain and Biswass 2017).

This improvement in hardness with the incorporation of filler was attributed to several factors. With particle-filled composites, the filler particles are distributed very close to one another and occupy the space between the matrix and the fibers. During the hardness test, a compressive load is applied to composite specimen. The matrix and the solid filler phase press together more tightly when a load is applied during the test. As a result, the specimen offers a resistance to penetration by the indenter (Pawar *et al.* 2015).

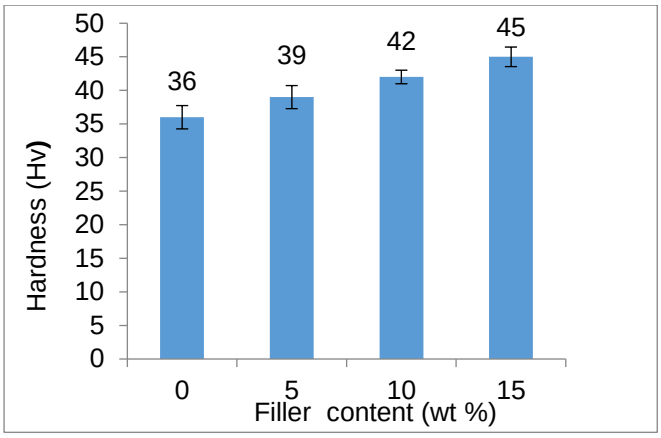

Fig. 1. Hardness with standard deviation of PLSS filled and unfilled palm-epoxy composite

Table 6. Mechanical Properties of PLSS Filled Palm-epoxy Composites

Composites	~Hardness (Hv) [S.D.]	~Tensile Strength (MPa) [S.D.]	~Flexural Strength (MPa) [S.D.]	~Impact Energy (J) [S.D.]
C_1	36 [1.74]	58.12 [1.80]	53.52 [1.56]	48 [1.49]
C_2	39 [1.72]	42.85 [1.50]	40.15 [1.76]	53 [1.13]
C_3	42 [1.01]	40.28 [1.70]	37.12 [1.47]	56 [1.39]
C_4	45 [1.46]	37.42 [1.08]	34.52 [1.61]	58 [0.93]

~: Average value; [S.D.]: Standard Deviation

Mechanical properties

Tensile strength

The tensile strengths with standard deviations of the palm-epoxy composites reinforced with different levels of PLSS powder are presented in Table 6 and shown in Fig. 2. The tensile strength gradually decreased as the filler powder level increased. The composite without PLSS had a tensile strength of 58.1 MPa; this value decreased to 42.8

MPa, 40.3 MPa, and 37.4 MPa as the PLSS powder addition to the composite was 5 wt%, 10 wt%, and 15 wt%, respectively. This observation may have been due to the poor interfacial bonding between the filler particles and the epoxy matrix, which promoted micro-cracks at the interfaces during the composite's loading as shown in Fig. 3. It shows pullout of fiber from the matrix with small cracks in the peripheral region. The other reason for the reduced tensile strength was the non-uniform stress distribution from the matrix to the fibers due to PLSS powder agglomeration within the matrix. The present resuls are consistent with previous investigators (Srivastava and Pawar (2006) for glass-epoxy composites filled with fly-ash, Biswas and Satapathy (2009) for glass-epoxy composites filled with red mud, Rout and Satapathy (2012) for glass-epoxy composites with rice husk particulates, and Jena *et al.* (2016) for bamboo-epoxy composites with ceno-sphere).

However, Joseph *et al.* (1996) observed enhancement in tensile strength of short sisal fiber reinforced with polyethylene composites. Similarly, Liu *et al*. (2014) found better tensile strength of abaca-epoxy composites than the untreated ones. This increment in tensile strength of the composites may be attributed to the chemical treatment and without any filler in the matrix.

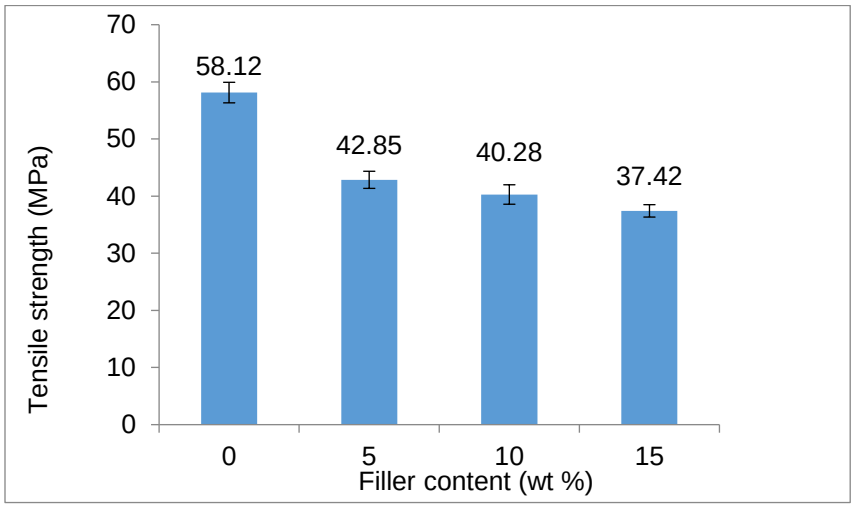

Fig. 2. Tensile strength with standard deviation of PLSS filled and unfilled palm-epoxy composite

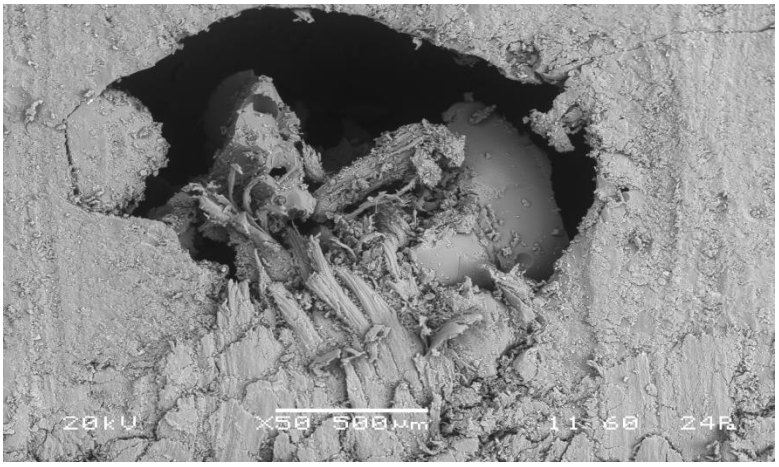

Fig. 3. SEM micrograph of C_3 composite showing fiber pullout and matrix crack

Flexural strength

Flexural strength of the palm-epoxy composites filled with PLSS powder is presented in Table 6 and Fig. 4. The bending strength of the composite gradually decreased with increasing filler addition. The flexural strength of the composite sample without PLSS powder was 53.1 MPa; this value decreased to 40.2 MPa, 37.1 MPa, and 34.5 MPa as the PLSS powder addition to the composite was 5 wt%, 10 wt%, and 15 wt%, respectively. Similar observations have been found earlier by previous investigators (Biswas and Satapathy (2009) for glass-epoxy composites filled with red mud, Rout and Satapathy (2012) for glass-epoxy composites with rice husk particulates, Rout and Satapathy (2013) for glass-epoxy composites filled with granite particles, and Biswas (2014) for bamboo-epoxy composites with copper slag as filler). This observed phenomenon was attributed to the poor dispersion of the filler particles within the matrix and to the greater existence of voids within the composite matrix. The presence of voids at the surfaces greatly reduced the composite's flexural strength in terms of delamination and fracture of fiber layers from the matrix. This is apparent in the SEM micro-graph shown in Fig. 5.

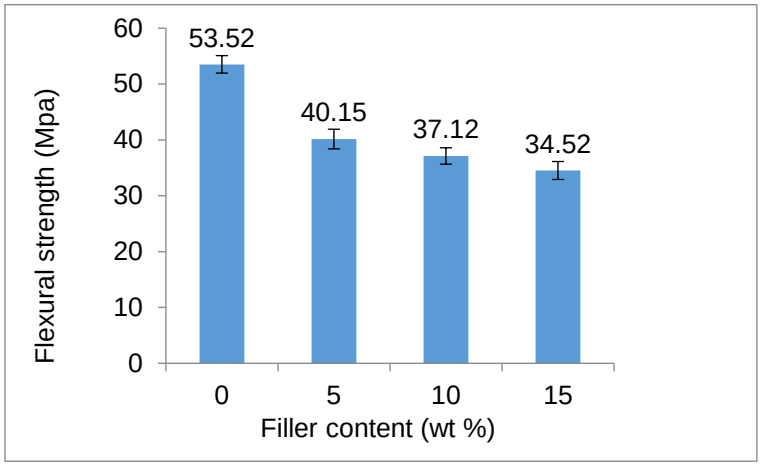

Fig. 4. Flexural strength with standard deviation of PLSS filled and unfilled palm-epoxy composite

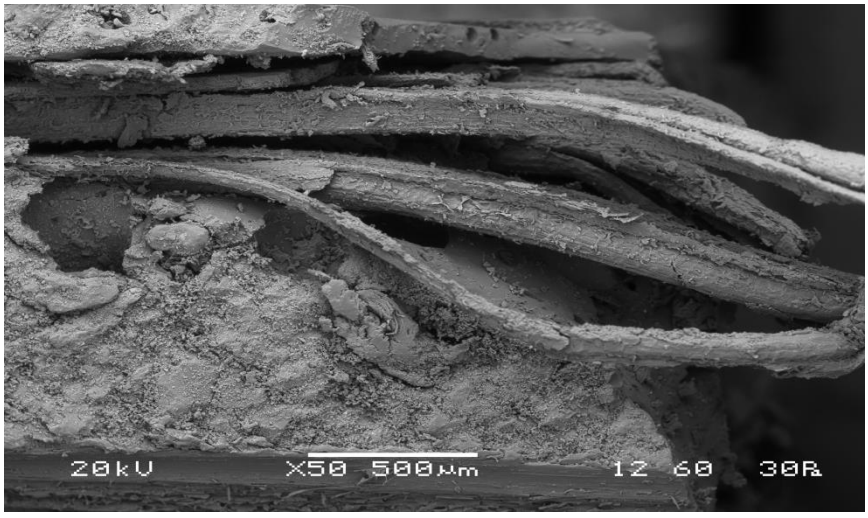

Fig. 5. SEM micrograph showing delamination and fracture of fiber of C_4 composite

Impact energy absorption

In many engineering applications, composite specimens are subjected to impact loads. Hence, it is essential to examine the impact energy absorption of the composites. Figure 6 shows the impact energy absorption of palm-epoxy composites filled with PLSS powder. It shows that the impact energy absorption of palm-epoxy composites increased with increasing powder addition to the composites. This observed behavior was attributed to the presence of PLSS powder at the interfacial regions, which reduced the bond strength between the fiber and matrix. With the weaker fiber-matrix interfaces, the composite broke into many parts when subjected to impact load, which resulted in more energy being absorbed, as evidenced in the SEM micrograph shown in Fig. 7. The present results are consistent with previous investigations of bamboo-epoxy composites filled with cement by-pass dust (CBPD) (Gupta *et al*. (2012), glass-epoxy composites filled with red mud (Biswas and Satapathy 2009), glass-epoxy composites with rice husk particulates (Rout and Satapathy 2012), glass-epoxy composites filled with granite particles (Rout and Satapathy 2013), and bamboo-epoxy composites with copper slag as filler (Biswas (2014).

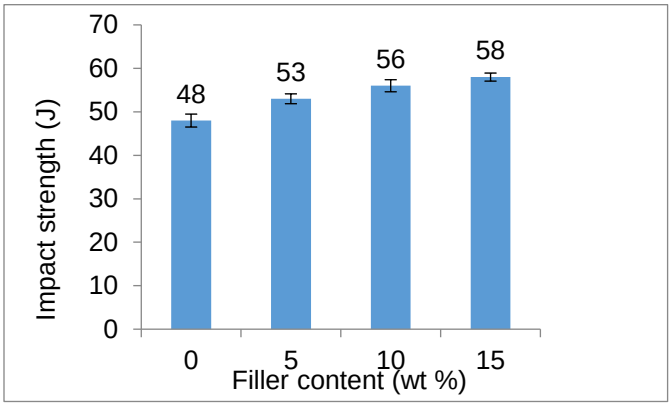

Fig. 6. Impact strength with standard deviation of PLSS filled and unfilled palm-epoxy composite

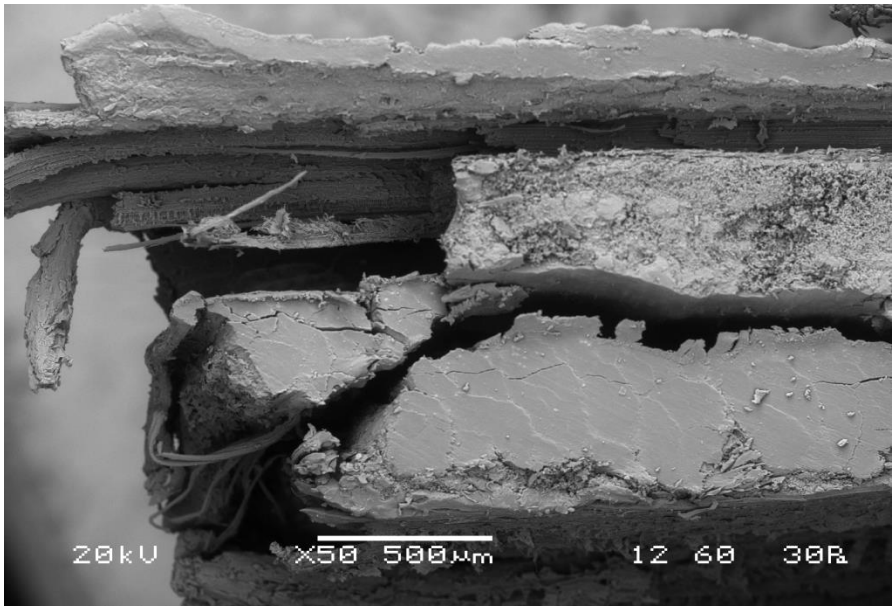

Fig. 7. SEM micrograph showing debonding and matrix cracks of C_3 composite

Erosion Test Results and Taguchi Analysis

Initial erosion tests

Table 4 shows the erosion rate of all 16 test runs along with the calculated S/N ratios. The mean value of the SN ratio for all 16 test runs was -51.84 dB. An analysis of the results indicated that a factor combination of A_2 (filler content of 5 wt%), B_1 (impact velocity of 40 m/s), C_1 (impingement angle of 45°), and D_3 (erodent size of 80 µm) resulted in the lowest erosion wear (Fig. 8). Furthermore, the order of control factors: impact velocity (B) (Rank-1), filler content (A) (Rank-2), impact angle (C) (Rank-3), and erodent size (D) (Rank-4), are in decreasing order according to their significance on the erosion rate and is presented in Table 7. Additionally, the erodent size had the smallest effect when compared to the other factors on the erosion rate.

Rout and Satapathy (2013) reported that the factor combinations of impact velocity (33 m/s), filler content (10 wt %), impingement angle (30º), and erodent size of (250 µm) in the decreasing order yielded minimum erosion for glass-epoxy composites filled with granite particulates. In another study, Rout and Satapathy found minimum erosion in the factor combinations of impact velocity (43 m/s), filler content (15 wt %), impingement angle (45º), and erodent size of (200) µm for glass-epoxy composites filled with rice-husk particles. Biswas and Satapathy (2009) mentioned that factor combinations of impact velocity (54 m/s), filler content (10 wt %), erodent temperature (30 ºC), impingement angle (30º), and stand-off distance (75 mm), in decreasing order, gave minimum erosion for glass-epoxy composites filled with red mud. Similarly, Biswas and Satapathy (2010) noticed that factor combinations of impact velocity (65 m/s), filler content (10 wt %), erodent temperature (30 ºC), impingement angle (90º), stand-off distance (75 mm), and erodent size (300 µm) in decreasing order yielded minimum erosion for glass-epoxy composites filled with alumina.

Impact velocity of the erodent is the most significant parameter in various investigations by the researchers. In general, the erodent has two components of velocity when it strikes the target material, that is, one tangential to the surface and the other normal to it. The normal component causes depth of penetration and determines the contact time. The product of contact time and tangential component of velocity creates the abrading distance in the material surface and the product of abrading distance and area of penetration causes volume of material loss. Therefore, the rate of material loss is directly proportional to the velocity of impact. However, the presence of filler particle in the matrix greatly reduces the velocity of erodent and as a result, the erosion rate of the material decreases significantly (Rout and Satapathy 2013).

From the reported results, it may be concluded that the erosion behavior of polymer composite with different fillers strongly depends on the experimental parameters such as impact velocity, impingement angle, stand-off distance, erodent size, erodent temperature, *etc.* or target related material property such as volume/weight fraction of fiber/filler, dispersion of filler in the matrix, orientation of fiber, type of matrix material and percentage of void content in the matrix, *etc.* It is also found that addition of filler into the matrix may increase the erosion resistance of the polymer composite, whereas in other investigations (Harsha *et al.* 2003), it has reduced the erosion resistance. Hence, one should properly decide the type and amount of filler into a matrix before any particular application.

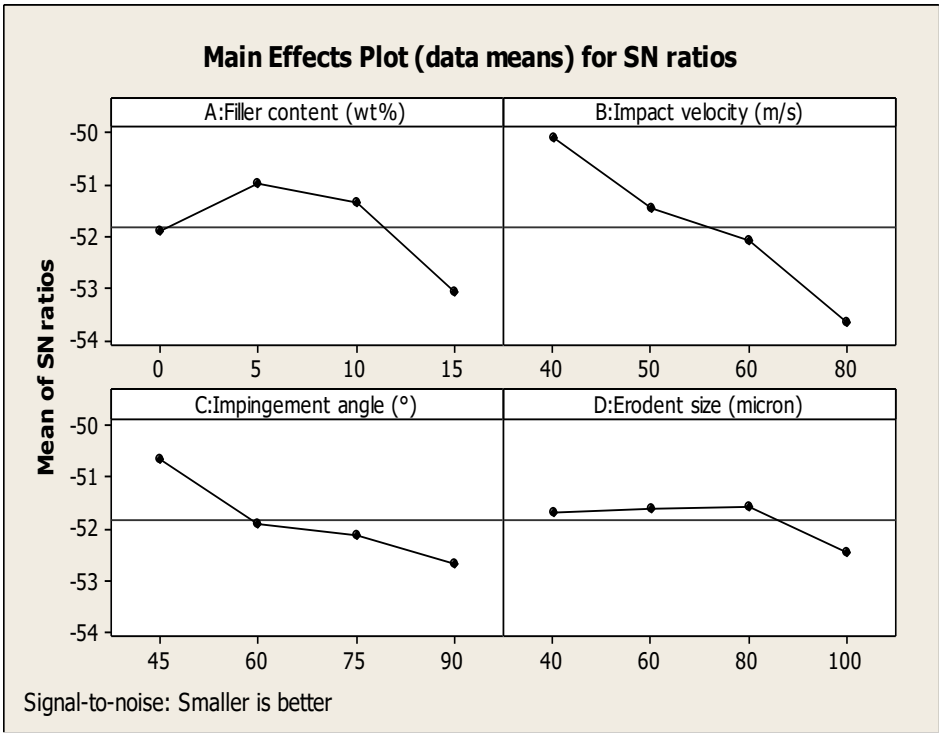

Fig. 8. Effects of control factors on erosion rate

Table 7. S/N Ratio Response Table for Erosion Rate

Level	A :(Filler Content)	B: (Impact Velocity)	C: (Impact Angle)	D: (Erodent Size)
1	-51.88	-50.11	-50.65	-51.70
2	-50.99	-51.47	-51.89	-51.60
3	-51.37	-52.08	-52.13	-51.57
4	-53.09	-53.67	-52.66	-52.46
Delta	2.10	3.56	2.01	0.88
Rank	2	1	3	4

Table 8. ANOVA for Erosion Rate

Source	DF	Seq. SS	Adj. SS	Adj. MS	F_0	*p*-value
A	3	20298.1	20298.1	6766.0	27.62	0.011
B	3	53914.5	53914.5	17971.5	73.37	0.003
C	3	15561.0	15561.0	5187.0	21.18	0.016
D	3	6056.4	6056.4	2018.8	8.24	0.058
Error	3	734.8	734.8	244.9		
Total	15	96564.8				

Note: degrees of freedom (DF); sum of squares (SS); mean of squares (MS); S = 15.6506; R^2 = 99.24%; R^2 (adj.) = 96.20%

ANOVA and the effect of factors

The statistical significances of the various control factors on the erosion rate were analysed by ANOVA (Table 8). The statistical significances were determined at the 95% confidence level. The *p*-value indicates if the independent factor has a significant probability of affecting the observed value.

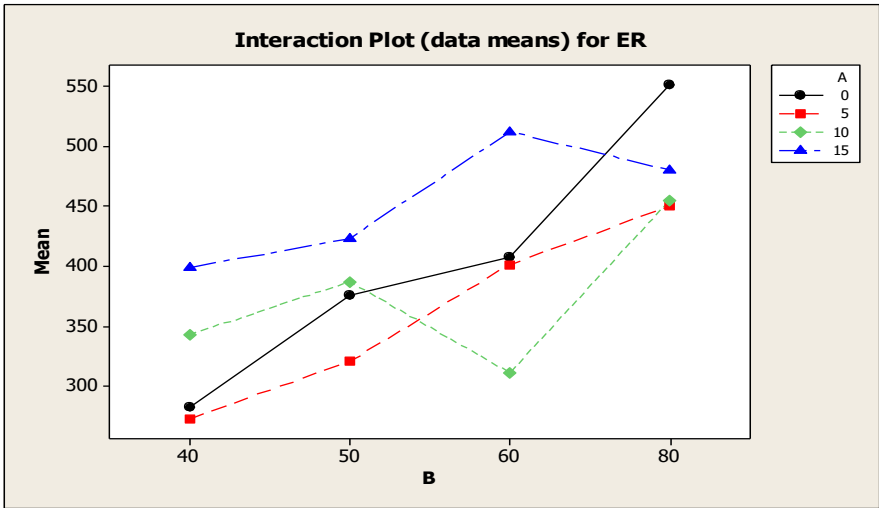

Fig. 9. Interaction graph between A×B for erosion rate

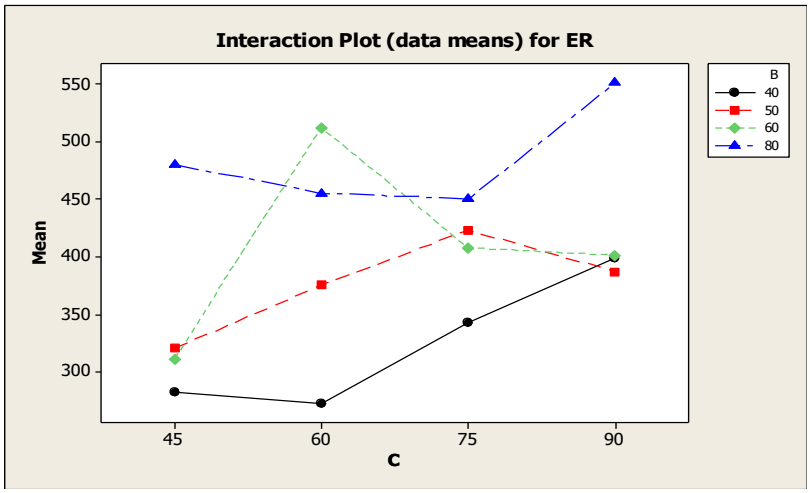

Fig. 10. Interaction graph between B×C for erosion rate

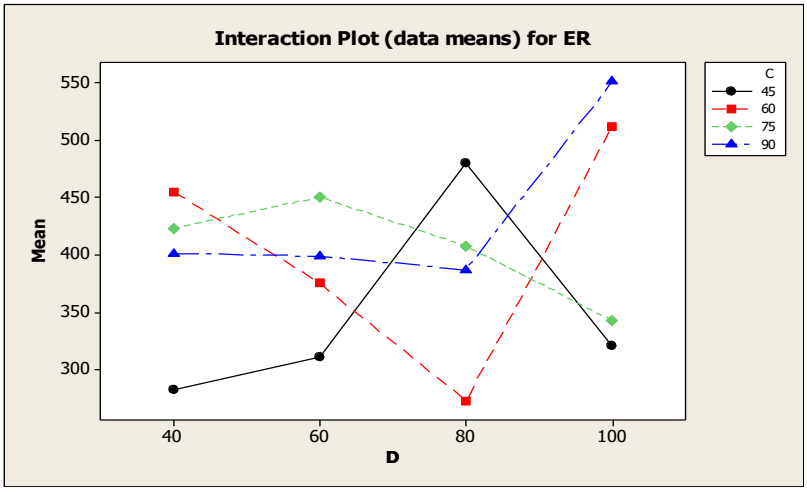

Fig. 11. Interaction graph between C×D for erosion rate

All factors had very small values of *p*. It was observed that the filler content (p = 0.011), impact velocity (p = 0.003), impingement angle (p = 0.016), and erodent size (p = 0.058) influenced the erosion rate. The interaction between the filler content and impact velocity (A × B; p = 0.000033) (Fig. 9), and impact velocity and impact angle (B × C; p = 0.000048) (Fig.10) significantly affected the erosion rate. The impact angle and erodent size interaction (C × D) had a minimum contribution on the erosion rate (p = 0.000928) (Fig. 11).

Confirmation experiments

The main idea behind the confirmation experiments was to verify the initial conclusions obtained from the earlier analysis. The erosion wear of the composites can be predicted by conducting a new set of factor settings ($A_1B_2C_2D_1$). A prediction equation can be developed using the Taguchi approach to estimate the SN ratio for erosion rate,

$$\bar{\eta}_1 = \bar{T} + (\bar{A}_1 - \bar{T}) + (\bar{B}_2 - \bar{T}) + (\bar{C}_2 - \bar{T}) + (\bar{D}_1 - \bar{T}) \quad (5)$$

where $\bar{\eta}_1$ is the predicted average, $\bar{T}$ is the overall experimental average, and $\bar{A}_1$, $\bar{B}_2$, $\bar{C}_2$, and $\bar{D}_1$ are the mean responses for the factors at the corresponding level denoted by the subscript. Equation 5 can be reduced by combining like terms to:

$$\bar{\eta}_1 = \bar{A}_1 + \bar{B}_2 + \bar{C}_2 + \bar{D}_1 - 3\bar{T} \quad (6)$$

The new arbitrary arrangement of factor levels A_1, B_2, C_2, and D_1 is used to predict the wear through the prediction equation (Eq. 6), and the SN ratio was calculated as -51.44 dB. An experiment was performed at A_1, B_2, C_2, and D_1. The result was compared with the predicted value from Eq. 7 (Table 9). The developed model predicted the erosion wear with a sensible accuracy level. The observed error between the predicted and experimental values was 3.45%. This error could be further reduced if the number of measurements is increased.

Table 9. Results of the Confirmation Experiment for Erosion Rate

	Optimal Control Parameter		**Error (%)**
	Prediction	Experimental	
Level Erosion Wear	A_1, B_2, C_2, D_1 -51.44 mg/kg	A_1, B_2, C_2, D_1 -49.73 mg/kg	3.45

Morphology of Eroded Samples

The erosion wear resistance of the composites mainly depends on experimental factors like impact velocity, impingement angle, erodent size, and material composition (Harsha *et al*. 2003). The effect of various factors on palm-epoxy composite filled with PLSS powder has been examined microscopically. The main objective of this phase of the study is to classify various modes of material removal from the composite's surface.

The microstructure of the C_1 composite surface that was eroded at an impact angle of 90° and impact velocity of 80 m/s is shown in Fig. 12. The figure illustrates that the matrix layer above the fiber surface has been chipped-off, and that the reinforcing fibers were broken. Small cracks were also observed in the micrographs. These observations were attributed to the repeated collisions of hard alumina particles (erodent) at high velocity, which caused an increase in the surface temperature that made it easier to remove the matrix at the composite's surface.

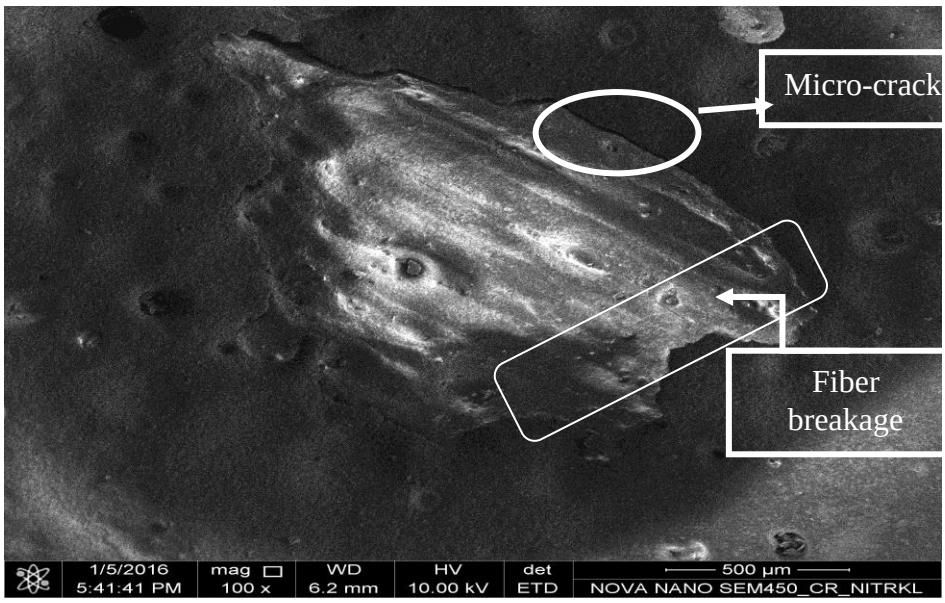

Fig. 12. Scanning electron micrograph of the eroded composite (C_1) at an impingement angle of 60° and impact velocity of 60 m/s

Figure 13 shows the micrograph of the C_4 composite when it was eroded at 80 m/s with an impingement angle of 45°. When the erodent strikes at an angle, it has two components, one parallel to the material's surface and the other perpendicular to the surface. The parallel component primarily removed material from the surface due to micro-plowing, which was observed in the micrograph. The normal component created a surface crater that made the surface rough, which was also observed in Fig. 13.

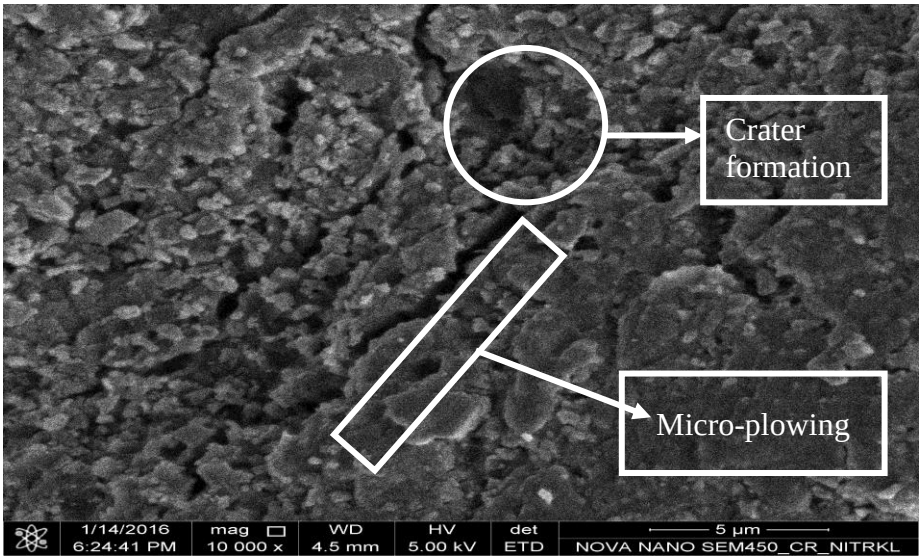

Fig. 13. Scanning electron micrograph of the eroded composite (C_4) at an impingement angle of 45° and impact velocity of 80 m/s

CONCLUSIONS

1. A new class of palm leaf stem-epoxy composite filled with palm leaf stem stalk (PLSS) powder has been successfully fabricated by simple hand-lay-up technique.
2. The experimental data revealed that the hardness and impact energy absorption of the palm-epoxy composites increased with increasing PLSS powder level, whereas the tensile and flexural strengths decreased.
3. The erosion study indicated that palm-epoxy composite filled with 15 wt% PLSS had the maximum erosion resistance when compared to other composite formulations.
4. Erosion wear characteristics of these composites were analyzed using the Taguchi experimental approach. The statistical analysis revealed that factors like impact velocity, filler content, impact angle, and erodent size were statistically significant in affecting the erosion rate (in decreasing order).
5. Microscopic observations of the eroded surfaces were examined at various experimental conditions. Several erosion wear mechanisms, such as crater formation, micro-plowing, fiber-matrix debonding, fragmentation, *etc*. were observed.

ACKNOWLEDGMENTS

The authors are grateful to the *BioResources* staff for their suggestions in rectification and modification of the manuscript. Authors would also like to thank Abhisek Choudhury, NIT Rourkela, India for his help during SEM of eroded samples and Dr. Prasanta Rath, Associate Professor, School of Applied Sciences, KIIT University, Bhubaneswar, India for his support during experimentation.

REFERENCES CITED

Agarwal, B. D., and Broutman, L. J. (1990). *Analysis and Performance of Fiber Composites*, 2nd Edition, John Wiley & Sons, New York, USA.

ASTM D256-10 (2010). "Standard test methods for determining the Izod pendulum impact resistance of plastics," ASTM International, West Conshohocken, PA.

ASTM D790-03 (2003). "Standard test methods for flexural properties of unreinforced and reinforced plastics and electrical insulating materials," ASTM International, West Conshohocken, PA.

ASTM D3039M-14 (2014). "Standard test method for tensile properties of polymer matrix composite materials," ASTM International, West Conshohocken, PA.

ASTM E384-11e1 (2011). "Standard test method for Knoop and Vickers Hardness of materials," ASTM International, West Conshohocken, PA.

ASTM G76-13 (2013). "Standard test method for conducting erosion tests by solid particle impingement using gas jets," ASTM International, West Conshohocken, PA.

Balaji, A. N., and Nagarajan, K. J. (2017). "Characterization of alkali treated and untreated new cellulosic fiber from Saharan aloe vera cactus leaves," *Carbohyd. Polym.* 174, 200-208. DOI: 10.1016/j.carbpol.2017.06.065

Biswas, S. (2014). "Erosion wear behaviour of copper slag filled short bamboo fiber reinforced epoxy composites," *International Journal of Engineering and Technology* 6(2), 91-94. DOI: 10.7763/IJET.2014.V6.672

Biswas, S., and Satapathy, A. (2009). "Tribo-performance analysis of red mud filled glass-epoxy composites using Taguchi experimental design," *Mater. Design* 30(8), 2841–2853. DOI: 10.1016/j.matdes.2009.01.018

Biswas, S., and Satapathy, A. (2010). "A study on tribological behavior of alumina-filled glass-epoxy composites using Taguchi experimental design," *Tribol. T.* 53(4), 520-532. DOI: 10.1080/10402000903491309

Boopathi, L., Sampath, P. S., and Mylsamy, K. (2012). "Investigation of physical, chemical and mechanical properties of raw and alkali treated Borassus fruit fiber," *Compos. Part B- Eng.* 43(8), 3044-3052. DOI: 10.1016/j.compositesb.2012.05.002

Das, G., and Biswas, S. (2017). "Erosion wear behavior of coir fiber-reinforced epoxy composites filled with Al_2O_3 filler," *J. Ind. Text.* 47(4), 472–488. DOI: 10.1177/1528083716652832

Dhakal, H. N., Zhang, Z. Y., and Richardson, M. O. W. (2007). "Effect of water absorption on the mechanical properties of hemp fibre reinforced unsaturated polyester composites," *Compos. Sci. Technol*. 67(7–8), 1674–1683. DOI: 10.1016/j.compscitech.2006.06.019

Fiore, V., Di Bella, G., and Valenza, A. (2015). "The effect of alkaline treatment on mechanical properties of kenaf fibers and their epoxy composites," *Compos. Part B-Eng.* 68, 14-21. DOI: 10.1016/j.compositesb.2014.08.025

Fung, K. L., Xing, X. S., Li, R. K. Y., Tjong, S. C., and Mai, Y. W. (2003). "An investigation on the processing of sisal fibre reinforced polypropylene composites," *Compos. Sci. Technol.* 63(9), 1255–1258. DOI: 10.1016/S0266-3538(03)00095-2

Gupta, A., Kumar, A., Patnaik, A., and Biswas, S. (2012). "Effect of filler content and alkalization on mechanical and erosion wear behavior of CBPD filled bamboo fiber composites," *Journal of Surface Engineered Materials and Advanced Technology* 2(3), 149-157. DOI: 10.4236/jsemat.2012.23024

Harsha, A. P., Tewari, U. S., and Venkatraman, B. (2003). "Solid particle erosion behaviour of various polyaryletherketone composites," *Wear* 254(7–8), 693-712. DOI: 10.1016/S0043-1648(03)00143-1

Jena, H., Pradhan, A. K., and Pandit, M. K. (2016). "Study of solid particle erosion wear behavior of bamboo fiber reinforced polymer composite with cenosphere filler," *Adv. Polym. Tech.* 37(3), 761-769. DOI: 10.1002/adv.21718

Jiang, L., He, C., Fu, J., and Li, X. (2018). "Wear behaviour of alkali-treated sorghum straw fiber reinforced polyvinyl chloride composites in corrosive water conditions," *BioResources* 13(2), 3362-3376. DOI: 10.15376/biores.13.2.3362-3376

John, M. J., Francis, B., Varughese, K. T., and Thomas, S. (2008). "Effect of chemical modification on properties of hybrid fiber biocomposites," *Compos. Part A- Appl. S.* 39(2), 352–363. DOI: 10.1016/j.compositesa.2007.10.002

Joseph, K., Thomas, S., and Pavithran, C. (1996). "Effect of chemical treatment on the tensile properties of short sisal fibre-reinforced polyethylene composites," *Polymer* 37(23), 5139-5149. DOI: 10.1016/0032-3861(96)00144-9

Ku, H., Wang, H., Pattarachaiyakoop, N., and Trada, M. (2011). "A review on the tensile properties of natural fiber reinforced polymer composites," *Compos. Part B- Eng.* 42(4), 856–873. DOI: 10.1016/j.compositesb.2011.01.010

Liu, K., Zhang, X., Takagi, H., Yang, Z., and Wang, D. (2014). "Effect of chemical treatments on transverse thermal conductivity of unidirectional abaca fiber/epoxy composite," *Compos. Part A- Appl. S.* 66, 227-236. DOI: 10.1016/j.compositesa.2014.07.018

Manimaran, P., Senthamaraikannan, P., Sanjay, M. R., Marichelvam, M. K., and Jawaid, M. (2018). "Study on characterization of *Furcrae foetida* new natural fiber as composite reinforcement for light weight applications," *Carbohyd. Polym.* 181, 650-658. DOI: 10.1016/j.carbpol.2017.11.099

Mohan, N., Mahesha, C. R., and Rajaprakash, B. M. (2013). "Erosive wear behaviour of WC filled glass epoxy composites," *Procedia Engineering* 68, 694–702. DOI: 10.1016/j.proeng.2013.12.241

Mohanta, N., and Acharya, S. K. (2015). "Mechanical and tribological performance of *Luffa cylindrica* fibre-reinforced epoxy composite," *BioResources* 10(4), 8364–8377. DOI: 10.15376/biores.10.4.8364-8377

Mohanty, J. R. (2017). "Investigation on solid particle erosion behavior of date palm leaf fiber- reinforced polyvinyl pyrrolidone composites," *J. Thermoplast. Compos.* 30(7), 1003-1016. DOI: 10.1177/0892705715614079

Obi Reddy, K., Uma Maheswari, C., Shukla, M., Song, J. I., and Varada Rajulu, A. (2013). "Tensile and structural characterization of alkali treated Borassus fruit fine fibers," *Compos. Part B- Eng.* 44(1), 433-438. DOI: 10.1016/j.compositesb.2012.04.075

Panda, P., Mantry, S., Mohapatra, S., Singh, S., and Satapathy, A. (2014). "A study on erosive wear analysis of glass fiber–epoxy–AlN hybrid composites," *J. Compos. Mater.* 48(1), 107-118. DOI: 10.1177/0021998312469239

Patnaik, A., Satapathy, A., Chand, N., Barkoula, N. M., and Biswas, S. (2010). "Solid particle erosion wear characteristics of fiber and particulate filled polymer composites: A review," *Wear* 268(1), 249-263. DOI: 10.1016/j.wear.2009.07.021

Pawar, M. J., Patnaik, A., and Nagar, R. (2015). "Investigation on mechanical and thermo-mechanical properties of granite powder reinforced epoxy composites," *Polym. Composite.* 38(4), 736-748. DOI: 10.1002/pc.23633

Prabhu, R., Rahul, M. P., Aeilias, A., Sunny, B., Alok, J., and Bhat, T. (2017). "Investigation of tribological property of coconut shell powder filled epoxy glass composites," *Am. J. Mater. Sci.* 7(5), 174-184. DOI: 10.5923/j.materials.20170705.10

Rout, A. K., Kar, J., and Jesthi, D. K. (2016). "Effect of surface treatment on the physical, chemical, and mechanical properties of palm tree leaf stalk fibers," *BioResources* 11(2), 4432-4445. DOI: 10.15376/biores.11.2.4432-4445

Rout, A. K., and Satapathy, A. (2012). "Study on mechanical and tribo-performance of rice-husk filled glass-epoxy hybrid composites," *Mater. Design* 41, 131-141. DOI: 10.1016/j.matdes.2012.05.002

Rout, A. K., and Satapathy, A. (2013). "Study on mechanical and erosion wear performance of granite filled glass-epoxy hybrid composites," *P. I. Mech. Eng. L- J. Mat.* 229(1), 38-50. DOI: 10.1177/1464420713499483

Sarkar, N., Sahoo, G., Khuntia, T., Priyadarsini, P., Mohanty, J. R., and Swain, S. K. (2017). "Fabrication of acrylic modified coconut fiber reinforced polypropylene biocomposites: Study of mechanical, thermal, and erosion properties," *Polym. Composite*. 38(12), 2852-2862. DOI: 10.1002/pc.23887

Srivastava, V. K., and Pawar, A. G. (2006). "Solid particle erosion of glass fibre reinforced fly ash filled epoxy resin composites," *Compos. Sci. Technol.* 66(15), 3021–3028. DOI: 10.1016/j.compscitech.2006.02.004

Swain, P. T. R., and Biswas, S. (2017). "Influence of fiber surface treatments on physico-mechanical behaviour of jute/epoxy composites impregnated with aluminium oxide filler," *J. Compos. Mater.* 51(28), 3909-3922. DOI: 10.1177/0021998317695420

Tewari, U. S., Harsha, A. P., Häge, A. M., and Friedrich, K. (2002). "Solid particle erosion of unidirectional carbon fibre reinforced polyetheretherketone composites," *Wear* 252(11-12), 992-1000. DOI: 10.1016/S0043-1648(02)00063-7

Zhang, L., Zhang, G., Chang, L., Wetzel, B., Jim, B., and Wang, Q. (2016). "Distinct tribological mechanisms of silica nanoparticles in epoxy composites reinforced with carbon nanotubes, carbon fibers and glass fibers," *Tribol. Int.* 104, 225-236. DOI: 10.1016/j.triboint.2016.09.001

Article submitted: May 10, 2018; Peer review completed: July 13, 2018; Revised version received: July 25, 2018; Accepted; July 27, 2018; Published: August 7, 2018.
DOI: 10.15376/biores.13.4.7212-7231